Solar Energy Materials 14 (1986) 269–287
North-Holland, Amsterdam

USE OF SOL–GEL THIN FILMS IN SOLAR ENERGY APPLICATIONS *

R.B. PETTIT and C.J. BRINKER

Sandia National Laboratories, Albuquerque, New Mexico 87185, USA

The sol–gel process uses metal alkoxides of network forming cations, such as Si, B, or Al, in alcohol/water solutions to form glass-like, polymeric networks in liquid solution. Thin films are formed by depositing the solution on a substrate by spinning, dipping or spraying. When the film is then heated to moderate temperatures (400–500 °C), dense glass films or stable porous films are obtained. The use of sol–gel thin films in four solar energy materials applications is discussed:

1. Encapsulation of black chrome solar selective coatings improved the high temperature thermal stability by a factor of 2.7.
2. Formation of porous, antireflection coatings on glass envelopes used in solar thermal collectors increased the solar transmittance of the glass from 0.91 to greater than 0.96.
3. Double-layer, antireflection coatings of SiO_2 and TiO_2 on silicon solar cells reduced the solar reflectance of the cells from 0.36 to 0.04 and thereby improved cell efficiencies by 50%.
4. Protective coatings applied to silvered stainless steel substrates were used to form structural solar mirrors. Solar averaged specular reflectance values of 0.90 to 0.91 were obtained.

1. Introduction

Sol–gel glass technology is a very inexpensive and simple process for producing thin glass coatings of various compositions on a variety of material surfaces [1]. The coatings are currently being studied for use as protective, dielectric, or optical coatings depending upon the preparation methods. For the past several years, we have been applying this coating technology to develop materials with application to various solar energy systems. This paper summarizes results in four different areas: (1) the use of a thin glass layer to protect black chrome solar selective coatings from oxidation at high temperatures (≈ 300 °C); (2) the application of a porous, low index film to antireflect glass surfaces and thereby improve their solar transmittance properties; (3) the application of high and low index coatings to antireflect silicon solar cells and thereby improve their operating efficiency; and (4) the use of a thin glass layer to protect a silvered, stainless steel sheet in order to obtain a structural, high-reflectance, solar mirror. Research into applications (1) and (3) has been completed, while areas (2) and (4) are still undergoing active investigation. After a general discussion of the sol–gel glass preparation process, the specific sol–gel processing techniques developed for each solar energy application will be presented.

* This work performed at Sandia National Laboratories supported by the US Department of Energy under Contract number DE-AC04-76-DP00789.

2. Sol-gel process

The sol-gel process uses metal alkoxides ($M(OR)_x$, where M = Si, B, Ti, Al, etc. and R is an alkyl group, e.g. CH_3, C_2H_5, C_3H_7, etc.) as glass precursors, catalyzed by an acid or base, in alcoholic solutions (< 100°C). The metal alkoxide is partially hydrolyzed and polymerized to form a 3-dimensional glass-like network in which multivalent metal atoms are linked together by difunctional bridging oxygen atoms (see fig. 1). When polymerization is extensive, the system gels. Prior to gelation, the system may be diluted to form a solution suitable for coating glass, ceramic or plastic substrates. Multicomponent glass compositions can be formed by mixing different metal alkoxides in the correct sequence: thus by mixing boron and silicon alkoxides, a borosilicate glass composition is formed. The gel composition can be further modified by adding non-network forming constituents (e.g. alkali earth elements) as solutions of acetates, nitrates or alkoxides. The polymer size and degree of branching in these solutions can be tailored for specific applications by controlling the water content, pH, temperature, dilution, and aging [2,3]. After coating deposition by dipping, spinning, or spraying, solvent evaporation during drying concentrates the solution of polymers, causing continued crosslinking, and ultimately resulting in gelation. Removal of the solvent leaves an interconnected porosity in the film, and the final pore size depends upon the polymer size and topology prior to film formation (see fig. 2). When this porous film is heated, any organic material is decomposed and the remaining porous glass structure collapses (sinters) to form a dense glass film. If the heat treatment temperature is maintained below the densification temperature, a porous, glass film remains which will have a lower effective index of refraction than that of the bulk glass material.

Some of the physical changes that occur in multicomponent borosilicate Na-Al-B-Si film and monolith during the densification process are shown in fig. 3. Note that whereas complete densification occurs above 600°C, shrinkage begins almost immediately. Because the film is strongly adherent to the substrate, all of the volume shrinkage accompanying densification occurs in the direction normal to the

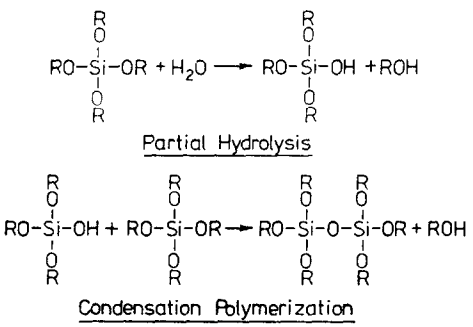

Fig. 1. Hydrolysis and condensation reactions that lead to the formation of a polymeric network in solution.

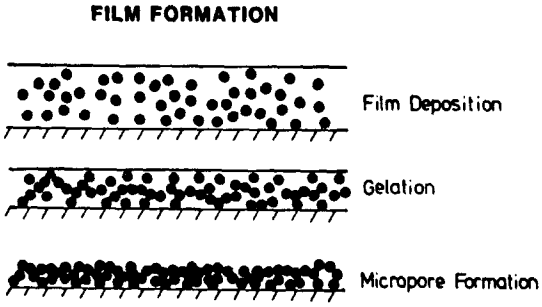

Fig. 2. A schematic showing micropore formation during gelation and solvent removal in a sol-gel thin film. The dots represent a polymeric cluster that formed in solution before deposition of the film.

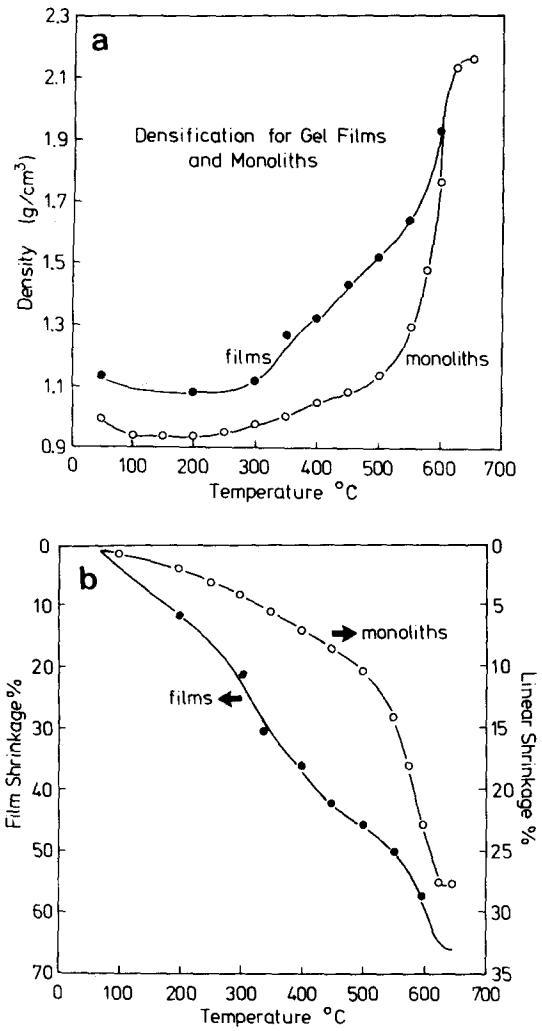

Fig. 3. Plot of the density (a) and % volume shrinkage (b) as a function of temperature for a multicomponent borosilicate sol-gel sample.

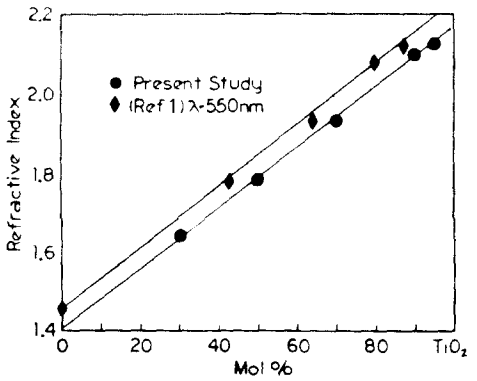

Fig. 4. The index of refraction measured at 632.8 nm for silica/titania thin film mixtures after heating to 400°C. Also shown are the results of ref. [1] measured at 550 nm.

substrate. Bulk gel specimens shrink isotropically. From the results shown in fig. 3, it can be seen that a dense glass is obtained at a temperature near the glass transition temperature of the corresponding melt-prepared glass, which is about 580°C for this particular composition.

The refractive index and thickness of a film can be controlled by varying the composition, the firing temperature, and the coating solution chemistry. For example, using a silica/titania mixture, the index of refraction can be continuously varied from about 1.4 to 2.2 [5] (see fig. 4). Since the mixing of the components occurs on a microscopic scale, the films are very homogeneous. For a single glass composition, the index starts at a low values due to the microporosity present and then increases

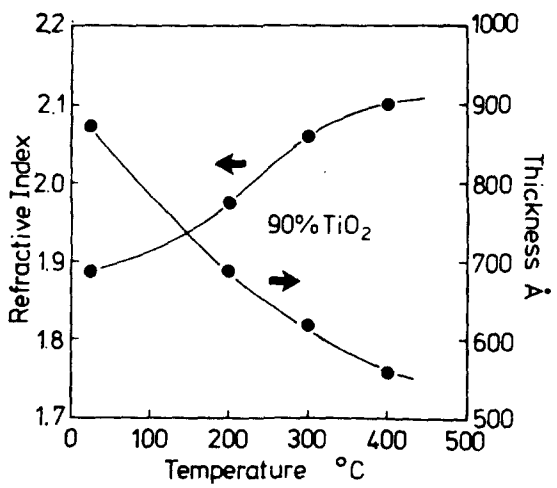

Fig. 5. The index of refraction and thickness of a 10% SiO_2/90% TiO_2 film as a function of heat treatment temperature.

as the film is densified (see fig. 5). Presently, index of refraction values cannot be varied below the value of the bulk glass if nonporous films are required.

3. Optical measurements

Spectral hemispherical reflectance and transmittance measurements were obtained using a Beckman model 5270 spectrophotometer with an integrating sphere accessory. Reflectance measurements of diffusely reflecting samples were referenced to National Bureau of Standards (NBS) diffuse reflectance standards, while reflectance measurements of mirror samples were referenced to NBS specular reflectance standards [6]. Both standards are accurate to 0.005 reflectance units. Specular reflectance measurements were obtained using a bidirectional reflectometer specifically designed for this purpose [7]. These measurements were also referenced to the NBS mirror standard. Emittance data were obtained using a Gier-Dunkle infrared reflectometer, model DB-100, as described in ref. [8].

4. Solar energy applications

4.1. Black chrome protective coatings

A solar selective coating must have a high solar absorptance and a low emittance. An electrodeposited black chrome coating consists of small particles (≈ 0.1 μm diameter) which are composed of small, metallic chromium crystals dispersed in an amorphous chrome oxide that appears to hold the film together [9] (see fig. 6). Because the coating is used in parabolic collectors that operate up to 300°C, the thermal stability of the coating is of utmost importance. By varying the electroplating process, the thermal stability can be substantially improved, but only by a limited amount [10]. It has been shown that the coating degrades by oxidation of the metallic chromium crystals [9]. Therefore, protecting the chromium from oxidation should increase the maximum operating temperature and lifetime of the coating.

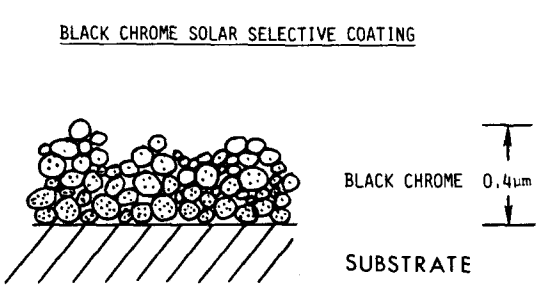

Fig. 6. Schematic diagram of the microstructure of electrodeposited black chrome showing the large (≈ 0.1 μm) particles that are composed of metallic chromium (dots) and amorphous chrome oxide.

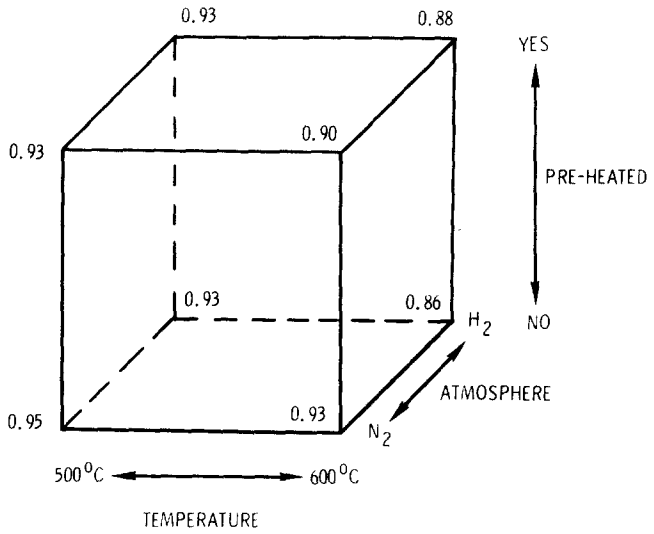

Fig. 7. Schematic representation of the effect of three sol–gel coating variables on the solar absorptance values measured for black chrome samples after aging for 100 h at 400°C in air.

The effect of applying a thin sol–gel coating to block chrome for this purpose was investigated [11].

For this study, there were six variables to control, including the sol–gel glass composition, the coating thickness, the heat treatment temperature, time and atmosphere, and whether the black chrome coatings were preaged (thermally heated) in order to build up a surface oxide layer to improve the sol–gel film bonding. In order to handle this large number of variables, an experimental design strategy was used to determine both the most important parameters affecting the thermal stability of coated samples and the range of these variables that provided a maximum benefit. Results for three of the variables mentioned above (firing temperature, firing atmosphere and preaging of the coating) are shown in fig. 7, where the three variables are plotted along perpendicular axes. Sol–gel coated black chrome films were processed according to the combination of variables specified at each of the eight vertices. The solar absorptance shown at each vertex was determined after accelerated aging of the coated samples for 100 h at 400°C in air. After this test the best coatings were obtained at the lower left front corner: a firing temperature of 500°C, the N_2 atmosphere, and on as-plated samples (no preaging). For an uncoated control sample, the solar absorptance decreased to a value of 0.89 after the same accelerated test. From the figure, it can be seen that the firing temperature had the largest affect on the thermal stability, with the atmosphere's effect next in importance, and the preaging last. Other experiments determined that borosilicate compositions performed better than coatings composed of silica/titania and silica/zirconia; that 500°C was the optimum firing temperature; and that a nitrogen atmosphere was better than dry hydrogen, air or vacuum. For the best

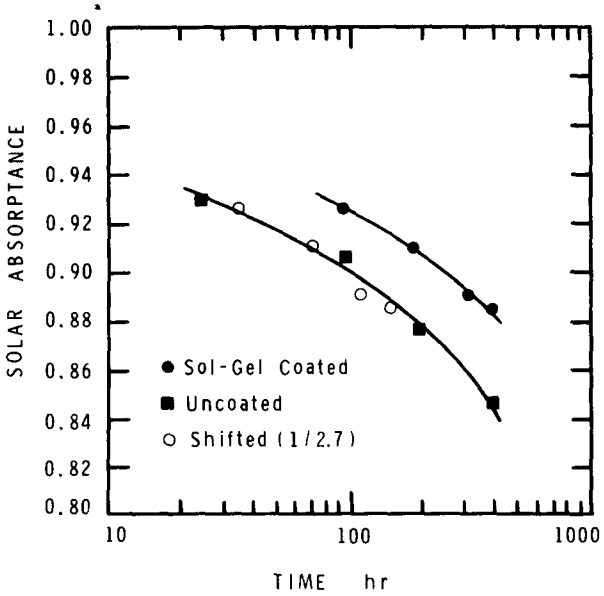

Fig. 8. The thermal aging behavior of both uncoated and sol–gel coated black chrome films as a function of time at 400°C. Also shown is the effect of shifting the sol–gel results by a factor of 0.37.

coatings, the increase in the emittance values for coated samples was less than 0.01–0.02 emittance units.

In order to determine the long term benefit of the best protective coatings, several coated samples, as well as uncoated control samples, were aged for longer times at 400°C. Solar absorptance values as a function of aging time are shown in fig. 8. Although the solar absorptance values continue to decrease with time for both samples, the solar absorptance of the sol–gel coated sample remains higher than that of the control sample. The aging results of both samples can be made to overlap by multiplying the heat treatment times for the coated sample by 0.37 ($= 1/2.7$). Thus it is possible to increase the lifetime of a coated sample by a factor of 2.7 as compared to an uncoated sample.

4.2. Antireflection coatings on glass

Most high temperature solar collectors utilize a glass envelope over the receiver surface to reduce convection and conduction losses. Reflection at the two glass/air interfaces results in a reduction in the solar transmittance by approximately 0.07 transmittance units. By antireflecting the glass, the solar transmittance can be increased from 0.91–0.92 to 0.97–0.98. One very effective way this can be accomplished with certain glass compositions is by the formation of a graded surface layer on the glass so that a smooth index of refraction match between the air and glass is achieved [12]. Formation of this layer is accomplished by heat treating at high temperature which allows the glass to separate into two phases of different composi-

tion. By selectively etching one phase, a graded index surface results. For Pyrex glass, it is necessary to heat treat the glass at 575°C for 24 h in order to cause the proper phase separation. However, this temperature is close to the softening point of the glass and deformation at these temperatures becomes a problem. Therefore the temperature must be kept to a minimum, which results in an increase in the heat treatment time. In addition, this process is limited to those glass compositions which will phase separate at high temperatures. Therefore, the use of porous sol–gel coatings to antireflect (AR) the glass was investigated.

As discussed earlier, the microstructure of an as-deposited sol–gel film can be varied by changing the type of polymer growth that occurs in solution before the film is deposited. It has been found that "aging" certain sol–gel solutions prior to film deposition results in increased pore volumes in the deposited film and thus a lower effective index of refraction. In particular, this phenomena has been found in sol–gel solutions with the following oxide composition (wt.%): 71% SiO_2; 18% B_2O_3; 7% Al_2O_3; 4% BaO. To investigate this effect, films were deposited on Pyrex slides using a dipping process. After coating, the films were heated to 500°C for relatively short times in order to partially solidify the film and form a durable but porous layer. After heating, the films were etched in a solution of 25 ml H_2SiF_6 and 0.75 g NH_4HF dissolved in 5475 ml H_2O.

For films deposited from freshly prepared solutions, the measured reflectance properties were approximately equal to those of the uncoated substrate. However, after aging the solution for 60 d at room temperature, the coating antireflected the substrate. The reflectance properties as-deposited and as a function of etching time are shown in fig. 9. The behavior of all curves can be adequately described by assuming that a single, uniform film of low index is deposited on the Pyrex. Note that the as-deposited film has a minimum reflectance of ≈ 0.02 at a wavelength of 900 nm, but as the etching progresses, the minimum reflectance decreases to values below 0.005 and shifts to lower wavelengths. After an etching time of 12 min, the solar averaged reflectance reaches a minimum value of 0.022 when the reflectance minimum is centered near 600 nm. By analyzing the spectral reflectance curves, the index of refraction and film thickness could be determined. The resulting values, plotted in fig. 10, show that the as-deposited film has an index of 1.35 and a thickness of 175 nm. As etching begins the index decreases rapidly and then remains relatively constant while the thickness initially remains constant and then begins to decrease. Therefore it appears that initially the pores in the film enlarge reducing the effective index, and then the thickness decreases shifting the reflectance minimum to lower wavelengths.

In order to determine the applicability of these coatings to a parabolic trough solar collector, a full-scale process was developed by Ashley and Reed [13] to antireflect 3.0 m long by 6.0 cm diameter received envelopes. To adapt the process for industrial use, the solution aging required to obtain the AR effect was accelerated by increasing the solution temperature. At 50°C, the optimum AR effect was obtained after only 14 d, as opposed to 60 d at room temperature. In order to coat the glass tubes, they were suspended inside a 7.6 cm diameter by 3.3 m long polyvinyl chloride pipe. The coating solution was pumped out of the pipe at a

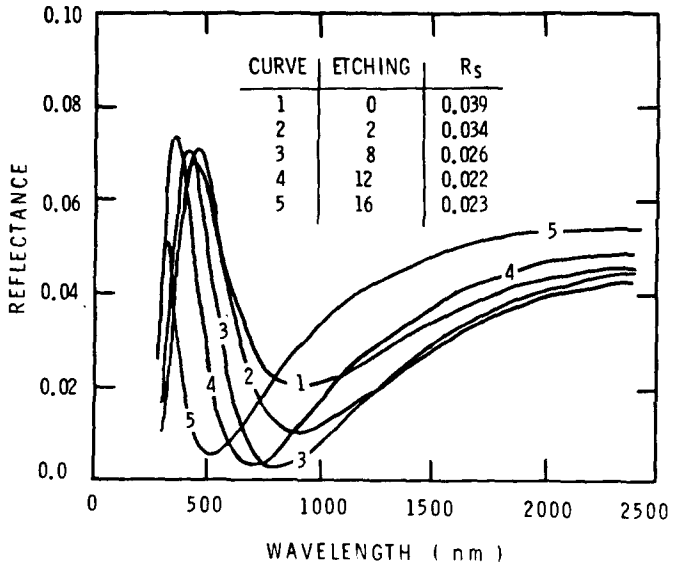

Fig. 9. The spectral reflectance properties of a sol-gel coated Pyrex slide both as-coated and after etching for times up to 16 min.

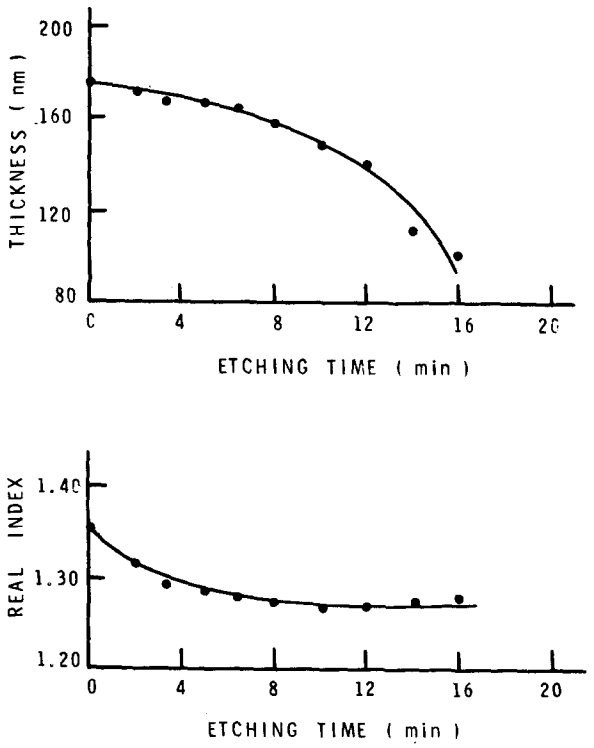

Fig. 10. The index of refraction and thickness of a sol-gel film on a Pyrex slide as a function of etching time as determined from spectral reflectance measurements.

constant speed and into a glass reservoir. After air drying the tubes with heat lamps, they were heated to 500°C in a conveyor belt furnace for only 12 min. The glass tubes were then etched, rinsed, dried and their optical properties determined. Solar averaged transmittance values ranged from 0.956 to 0.968 for 12 samples, with maximum end-to-end variations of ± 0.006. After processing, a gradual decrease in the transmittance was noted, which was attributed to absorption of water in the porous surface. However, after only a few minutes at 150°C, the transmittance increased to original values. Twelve tubes were installed at the Modular Industrial Solar Retrofit (MISR) test facility at Sandia, and after 16 weeks of operation the transmittance values of the envelopes had not changed to within the reproducibility (± 0.002) of the instrumentation for the measurements. Therefore this process was successful in coating full-scale receiver envelopes and showed no significant decrease in transmittance after extended outdoor operation [11].

4.3. AR coatings on silicon solar cells

Silicon solar cells have a high index of refraction which leads to a solar averaged reflectance value equal to about 36%. This large loss can be significantly reduced by coating the silicon with a thin, transparent dielectric layer with an appropriate dielectric constant and thickness. Single-layer AR coatings have included SiO, SiO_2, TiO_2, Si_3N_3, Ta_2O_5 and Al_2O_3, which lead to average reflectance values of only 10–12%. Further reduction in the reflectance can be accomplished with double-layer AR coatings. Therefore, double layers of SiO_2 and TiO_2, produced using sol–gel processing, were used to antireflect silicon solar cells [15].

The sol–gel SiO_2 and TiO_2 solutions were applied to 5 cm diameter, polished, n-type, phosphorus doped silicon wafers using a photoresist spinner. The thickness of the fired coatings could be adjusted by varying the rotation speed. The thickness of TiO_2 required for optimum optical properties could be applied through a single coating operation, while two coating operations were required for the SiO_2 film. Multiple coats were applied with only heat lamp drying between coatings. Samples were then fired at 450°C for 5 min to densify the individual layers. Samples of the individual coatings were also prepared for measurement of the index of refraction and thickness using ellipsometry at 632.8 nm. These values were then used in an optical modeling code to calculate the spectral reflectance properties.

Calculated and measured reflectance results for single coatings of SiO_2 and TiO_2, and a double-layer coating of the same films are shown in fig. 11. Note that the measured index for the SiO_2 coatings of 1.414 is slightly lower than the published value for fused silica of 1.457 (both at 632.8 nm). This indicates that the film is probably slightly porous. The agreement between the measured and calculated curves is excellent in all cases. For the double-layer coating, the solar averaged reflectance is only 0.049. Because of the excellent agreement between the measured and calculated results, the optical modeling code was used to determine the optimum thickness of each coating that minimized the solar reflectance. Calculations were performed using the measured index values and the resulting solar averaged properties were fit with a contour plot as shown in fig. 12. Note that the

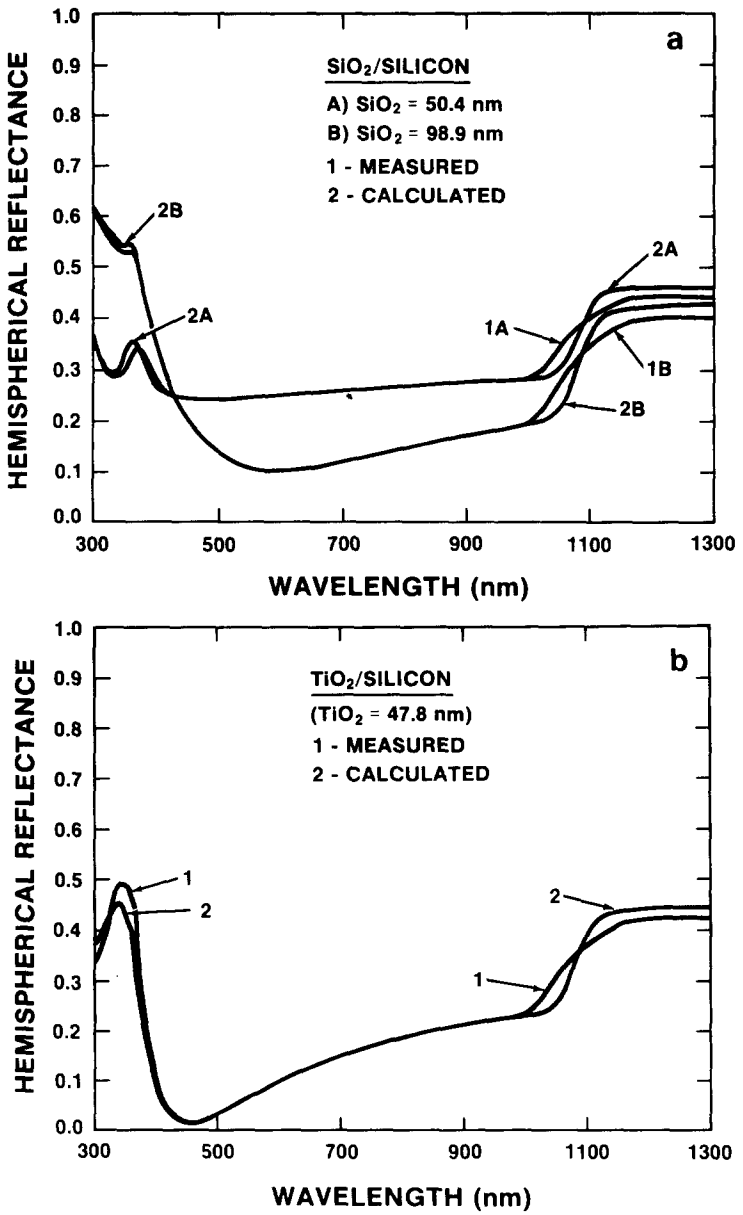

Fig. 11. Comparison of the measured and calculated spectral reflectance properties of (a) SiO_2, (b) TiO_2, and (c) SiO_2/TiO_2 sol-gel films deposited on silicon substrates.

minimum reflectance value of 0.038 is about 0.08 lower than a single-layer AR coating. This optimum sol-gel double-layer coating has a SiO_2 thickness of 95 nm and a TiO_2 thickness of 62 nm. It can also be seen from the figure that the

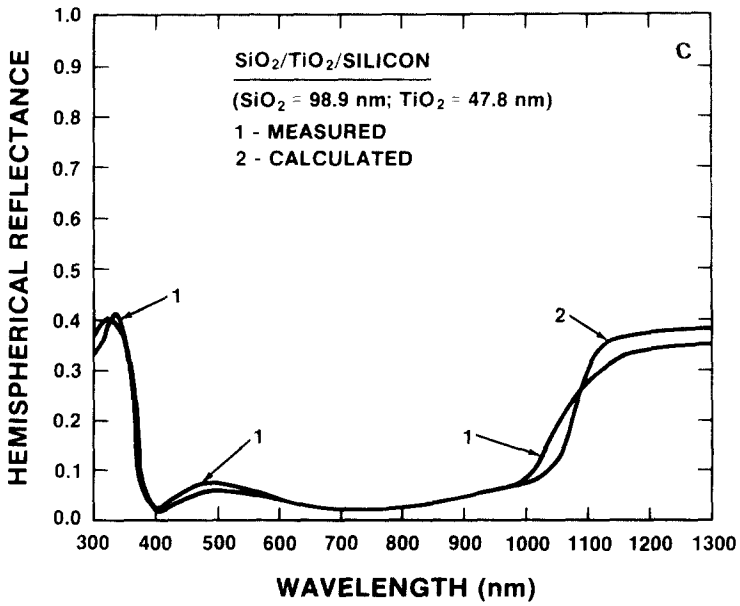

Fig. 11c. Caption on previous page.

reflectance is not very sensitive to thickness variations in the two films. Thus an increase in reflectance of only 0.01 above the optimum value (e.g. from 0.038 to 0.048) results from SiO_2 thickness variations of ± 25 nm and from TiO_2 thickness variations of ± 10 nm.

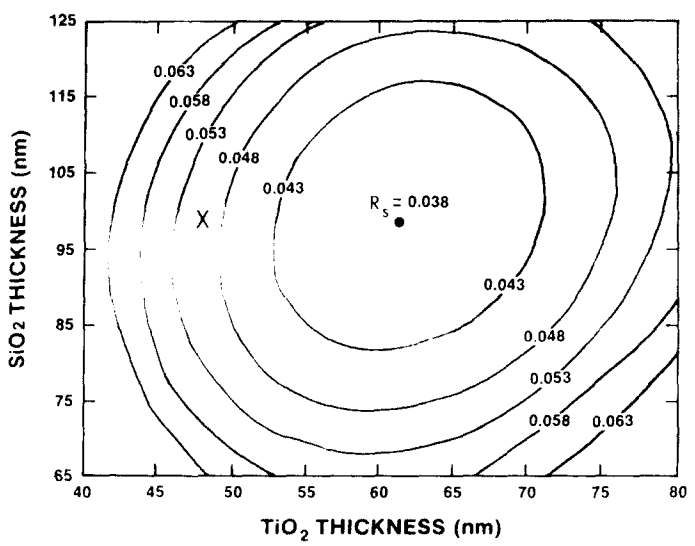

Fig. 12. Contour plot of the solar reflectance of double-layer sol-gel coatings on silicon as a function of the SiO_2 and TiO_2 film thickness.

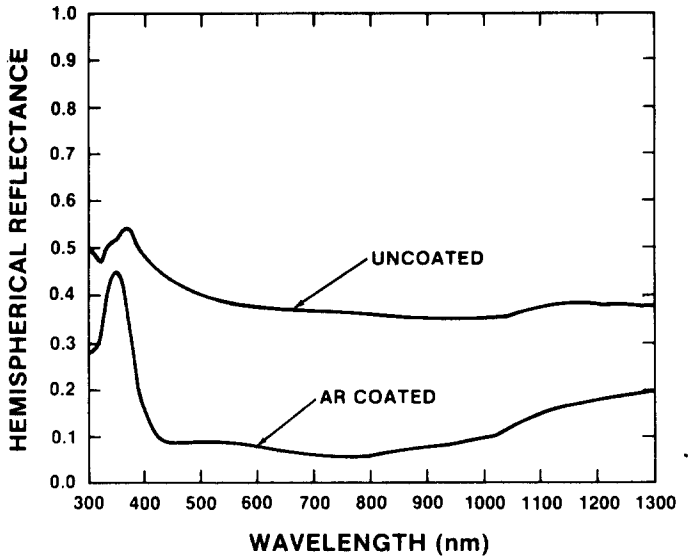

Fig. 13. Measured spectral reflectance properties of a Sandia solar cell both as-received and when coated with a double-layer sol–gel coating.

In order to determine if the decrease in reflectance corresponds to an equal increase in the cell efficiency, the performance of a Sandia designed solar cell was determined both before and after coating with the sol–gel double-layer coating. The reflectance properties of an uncoated and coated cell are shown in fig. 13. For the coated cell, the solar reflectance is 0.079, while the uncoated cell has a solar reflectance of 0.374. Thus the coating increased the cell solar absorptance from 0.626 to 0.921, or an increase of 47%. The measured cell efficiency increased from 12.1% to 17.4% for an increase of 44%. Because of the excellent agreement between the increase in absorptance and cell efficiency values, it appears that the 450°C firing temperature had no detrimental effect on the cell performance. Based on the measured reflectance of uncoated silicon of 0.36 and the minimum reflectance values possible of 0.028, it should be possible to increase the efficiency of a solar cell by slightly over 50% by using a sol–gel double-layer coating.

4.4. Solar mirror development

In solar concentrator applications that utilize reflectors to concentrate sunlight, the solar reflectance, the overall mirror shape and environmental stability of the mirror material are of utmost importance [16]. Currently, the mirror material that combines the best of these properties is silvered glass. By using a low iron content glass or a very thin glass, the solar reflectance can equal values from 0.92 to 0.97. When properly protected, glass mirrors show excellent environmental stability. Unfortunately, forming glass to the one or two dimensional curved shapes required in parabolic trough or dish concentrators can require costly and lengthy processing.

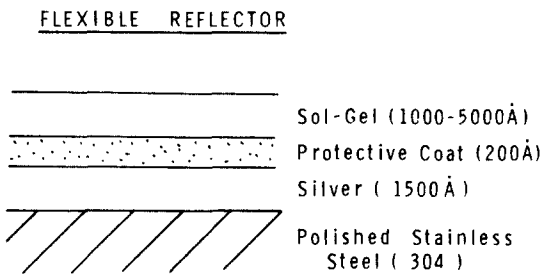

Fig. 14. Schematic of the flexible mirror concept being investigated by Sandia.

Therefore the development of a mirror material which can be easily processed into the required shape and which has a high solar reflectance and environmental stability is extremely desirable. One approach, that is being pursued by 3M Company and the Solar Energy Research Institute (SERI), is to silver a thin, transparent polymeric film that can be laminated to a smooth metal sheet [17,18]. 3M Company produces two silvered polymeric materials, ECP-94 and ECP-300X, which utilize an acrylic layer to protect the silver reflecting film and have solar reflectance values of 0.96 and 0.95, respectively.

The structural mirror concept that is being pursued at Sandia consists of a silvered, stainless steel sheet that is protected with a layer of sol–gel glass as shown in fig. 14. Initial experiments utilized a 304 stainless steel sheet that was polished to a mirror finish. After sputter cleaning, a nominal 150 nm thick silver layer was sputtered onto the stainless steel. Next an optional dielectric layer was added in order to protect the silver film during the sol–gel firing process; the dielectric chosen for preliminary tests was sputter deposited SiO_x. Finally a sol–gel protective glass layer was deposited on top of the composite to provide environmental protection. While research on this reflector has just begun, preliminary results have been encouraging. Initial experiments have concentrated on determining the best combination of sol–gel glass compositions, processing variables, need for an intermediate protective layer, and accelerated testing conditions.

Initial samples were prepared both with (protected) and without (bare) the protective SiO_x dielectric layer. Sol–gel glass compositions of TiO_2, SiO_2, and a 4-component borosilicate glass were applied using a dipping process. After coating, the samples were fired at temperatures ranging from 350°C to as high as 750°C in both nitrogen and vacuum environments. The hemispherical, diffuse and specular reflectance properties were determined as previously described [16]. Some typical results and the conclusion of this initial work are summarized below.

All coatings with TiO_2 composition suffered from the appearance of absorption bands which decreased the solar averaged reflectance values. The reflectance properties of a single-layer coating of TiO_2 prepared from an HCl catalyzed solution are shown in fig. 15. Note the strong absorption band at 500 nm and the weaker band at 1400 nm that are more pronounced for the bare silver than for the protected silver. The solar averaged hemispherical reflectance values of 0.86 and 0.92 are

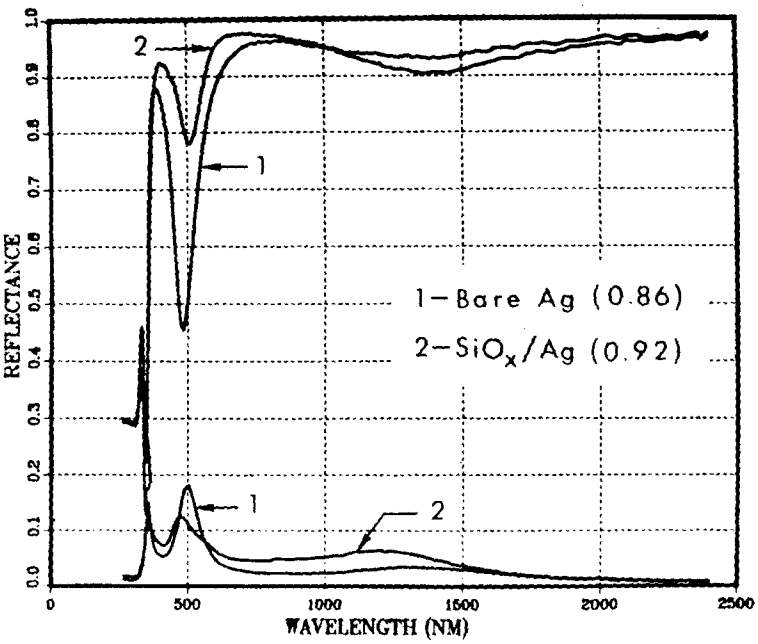

Fig. 15. The hemispherical and diffuse reflectance properties of TiO_2 coated mirrors. For curve 1 the sol-gel coating was desposited directly on bare silver, while for curve 2, a protective SiO_x layer was interposed.

substantially lower than the value obtained for the SiO_x protected and bare silver of 0.97. In addition, the amount of scattering, as indicated by the diffuse reflectance, shows a marked increase exactly where the absorption bands are a maximum.

Better results were obtained for the SiO_2 and 4-component sol-gel glass compositions as shown in fig. 16. Again sol-gel films deposited with the dielectric barrier on the silver were better than films deposited directly on the silver. For the samples shown, the solar average hemispherical reflectance values were 0.96 and 0.90. As with the TiO_2 coating, samples with reduced hemispherical reflectance values also display increased diffuse reflectance properties. Typical specular reflectance characteristics measured for an SiO_2 coated mirror are shown in fig. 17 together with results for the 3M silvered polymeric materials mentioned earlier. Note that the silvered stainless steel mirror reaches its asymptotic value by 2–3 mrad, while the ECP-94 reaches a constant value by 3 mrad and the ECP-300X by 5 mrad. However, the ECP-94 has the highest reflectance value of 0.96, followed by the ECP-300X at 0.95 and the silvered stainless steel at 0.90. By reducing the residual rolling marks on the stainless steel, the specular reflectance value at large angular apertures could be improved.

In order to determine the environmental protection afforded by the sol-gel coatings, samples were initially exposted to accelerated temperature/humidity cycle

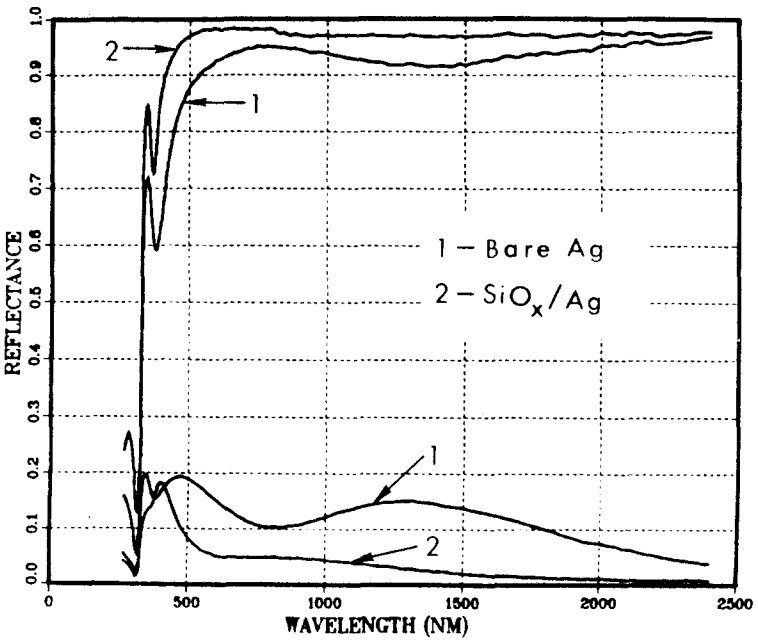

Fig. 16. The hemispherical and diffuse reflectance properties of 4-component sol–gel coated mirrors. For curve 1, the sol–gel coating was deposited directly on bare silver, while for curve 2 a protective SiO_x layer was interposed.

testing. The aging consisted of alternating high temperature (13°C to 54°C) and low temperature (−29°C to 13°C) cycles as previously described [19]. After 1 month of testing, no change was observed in the specular reflectance properties. In order to provide a more rapid test, samples were exposed to a 5% salt fog environment for 48 h. This test was designed only to provide a relative ranking of the various samples and was not designed as an accelerated outdoor aging environment. After the exposure, severe edge corrosion of the stainless steel had occurred. Where the silver and stainless were exposed to the salt environment, the stainless steel protected the silver and thus corroded rapidly. The corrosion products covered the mirror completely. Therefore, the test severity was reduced to a 0.5% salt fog. It was also realized that a dielectric barrier between the stainless steel and the silver would significantly reduce the galvanic corrosion that would occur in areas where the silver was exposed.

Results after exposure to a 0.5% salt fog for 48 h are summarized in table 1. For these tests the edges of the samples were protected with a glyptol paint. In all samples, cracks in the sol–gel film were visible although the specular reflectance properties decreased only a few percent for the 4-component and SiO_2 compositions. For the TiO_2 coatings, the specular reflectance dropped substantially and severe cracking in the coating was evident.

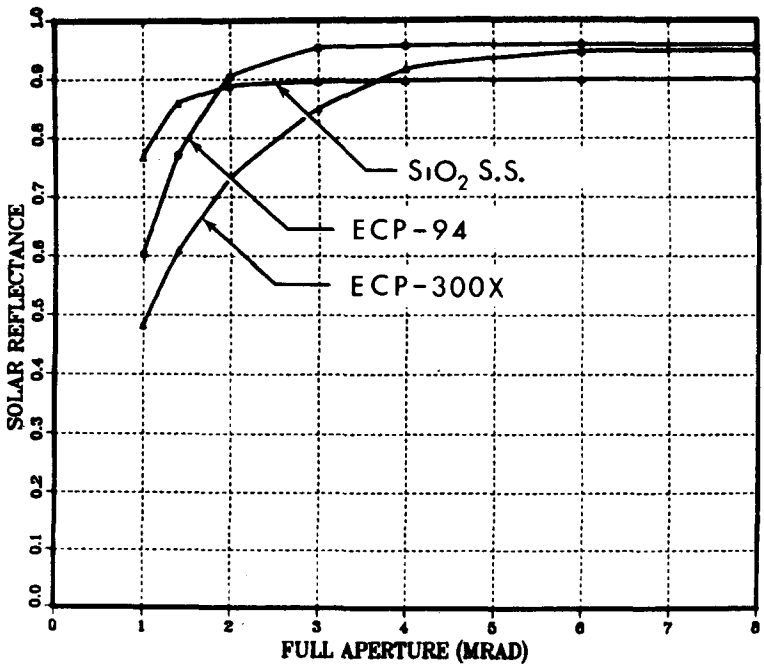

Fig. 17. The solar averaged specular properties of a SiO_2 coated stainless steel mirror together with two silvered polymeric mirrors manufactured by 3M Company: ECP-94 and ECP-300X.

Based on these results, the following conclusions have been obtained:

1. A dielectric, protective coating is required between the silver and sol–gel films to maintain high reflectance values and keep scattering to a minimum.
2. Films deposited on the 300 series stainless steel exhibited numerous cracks after processing. By switching to a 400 series stainless steel, the thermal expansion coefficient can be reduced by 40%.
3. A dielectric barrier between the stainless steel and silver layers will substantially reduce any galvanic corrosion at pin holes or cracks in the protective films.

Table 1
Results of 0.5% salt fog exposure accelerated testing for 48 h

Sol–gel	Results
SiO_2	0.01 specular reflectance loss
	Crack patterns visible
	Some brown corrosion products
4-Component	0.0 to 0.05 specular reflectance loss
	Some pinholes and crack visible
	Brown corrosion near edges
TiO_2	0.11 to 0.29 specular reflectance loss
	Severe cracking
	Brown corrosion products

4. The 4-component and SiO_2 sol–gel compositions produce comparable results. The TiO_2 composition resulted in strong absorption bands, enhanced scattering, and did not perform well in the salt fog testing.
5. The solar averaged specular reflectance properties are currently limited to values near 0.90 to 0.91 due to the intrinsic roughness of the strainless steel. Improved specular reflectance values could be obtained by smoothing the substrate material before coating.

5. Conclusions

Sol–gel thin films were used successfully in four solar energy applications as optical or protective coatings. By applying a thin layer over electrodeposited black chrome solar selective films, their thermal stability at high temperature was improved by a factor of 2.7. Optimized processing variables include heating to 500°C in a nitrogen atmosphere using a borosilicate sol–gel glass composition. Increase in the emittance of the coatings were less than 0.01–0.02 emittance units.

Antireflection coatings on glass were obtained using aged solutions of a 4-component borosilicate glass composition. After aging, deposited coatings displayed index of refraction values lower than values for the bulk glass. By acid etching the coatings, the index of refraction and thickness could be optimized to increase the solar transmittance to values near 0.96. Full scale parabolic trough receiver envelopes were processed and successfully operated in the MISR test facility at Sandia.

Using SiO_2 and TiO_2 thin films, the reflectance of silicon solar cells was reduced from 0.36 to values near 0.04. Based on the measured index of refraction values, the optimum film thicknesses were determined to be 95 nm for the SiO_2 film and 62 nm for the TiO_2 film. Applying this coating to a Sandia solar cell improved the operating efficiency by 44%, which was in excellent agreement with the measured increase in solar absorptance of 47%.

Finally, sol–gel films were used to protect silvered stainless steel mirrors. While solar averaged hemispherical reflectance values of 0.96 were obtained for SiO_2 and 4-component sol–gel glass compositions, the solar averaged specular reflectance was reduced to values near 0.90–0.91 due to the intrinsic roughness of the stainless steel substrate. TiO_2 sol–gel coatings suffered from both low solar reflectance values and limited environmental protection as determined in salt fog exposure testing. Additional work is required in order to optimize the coating process for this application.

References

[1] H. Schroeder, in: Physics of Thin Films: Advances in Research and Development, eds., G. Haas and R.E. Thun, 5 (1969) 87.
[2] C.J. Brinker, K.D. Keefer, D.W. Schaefer and C.S. Ashley, J. Non-Cryst. Solids 48 (1982) 47.
[3] C.J. Brinker, D.M. Haaland and R.B. Pettit, Annual Meeting of American Ceramic Society, Chicago, I1 (April, 1983).

[4] C.J. Brinker and R.B. Pettit, Sandia National Labs. Report SAND 83-0137 (March, 1983) pp. 68–80*.
[5] C.J. Brinker and M.S. Harrington, Solar Energy Mater. 5 (1981) 159.
[6] NBS White Ceramic Tile SRM 2019 and Second Surface Aluminum Mirror SRM 2023, obtained from NBS, Office of Standard Reference Materials, Washington, DC 20234, USA.
[7] R.B. Pettit, Solar Energy 19 (1977) 733.
[8] R.B. Pettit, J. Eng. Power 100 (1978) 489.
[9] J.N. Sweet, R.B. Pettit, and M.B. Chamberlain, Solar Energy Mater. 10 (1984) 251.
[10] R.B. Pettit, R.R. Sowell and I.J. Hall, Solar Energy Mater. 7 (1982) 153.
[11] R.B. Pettit and C.J. Brinker, SPIE–Optical Coatings of Energy Efficiency and Solar Appl. vol. 324 (1982) 176.
[12] H.L. McCollister and R.B. Pettit, J. Solar Energy Eng. 105 (1983) 425.
[13] C.S. Ashley and S.T. Reed, Sandia National Labs. Report SAND 84-0662 (Sept. 1984) *.
[14] C.P. Cameron, in: Proc. Distributed Receiver Solar Thermal Technology Conf. Albuquerque, NM (April 24–25, 1985) Sandia National Labs. Report SAND 84-2454 (April 1985) p. 261 *.
[15] R.B. Pettit, C.J. Brinker and C.S. Ashley, Solar Cells 15 (1985) 267.
[16] R.B. Pettit and E.P. Roth, Solar Materials Science, ed., L.E. Murr (Academic Press, New York, 1980) Chapter 5.
[17] P. Schissel, H.H. Neidlinger and A.W. Czanderna, Solar Energy Research Institute Report SERI/PR-255 2493 (Sept. 1984) *.
[18] B.A. Benson, Proc. Solar Thermal Annual Research Conf. Lakewood, CO (Feb. 20–22, 1985) to be published.
[19] A.R. Mahoney, R.B. Pettit, G.S. Konoshita, Sandia National Labs. Report SAND 84-0532 (Oct. 1984) *.

* Available from NTIS, US Department of Commerce, 5285 Port Royal Rd., Springfield, VA 22161.